FULL PAPER

Electrically Tunable Goos–Hänchen Effect with Graphene in the Terahertz Regime

Yuancheng Fan,* Nian-Hai Shen, Fuli Zhang, Zeyong Wei, Hongqiang Li, Qian Zhao, Quanhong Fu, Peng Zhang, Thomas Koschny, and Costas M. Soukoulis

Goos–Hänchen (G–H) effect is of great interest in the manipulation of optical beams. However, it is still fairly challenging to attain efficient controls of the G–H shift for diverse applications. Here, a mechanism to realize tunable G–H shift in the terahertz regime with electrically controllable graphene is proposed. Taking monolayer graphene covered epsilon-near-zero metamaterial as a planar model system, it is found that the G–H shifts for the orthogonal s-polarized and p-polarized terahertz beams at oblique incidence are positive and negative, respectively. The G–H shift can be modified substantially by electrically controlling the Fermi energy of the monolayer graphene. Reversely, the Fermi energy dependent G–H effect can also be used as a strategy for measuring the doping level of graphene. In addition, the G–H shifts of the system are of strong frequency-dependence at oblique angles of incidence, therefore the proposed graphene hybrid system can potentially be used for the generation of terahertz "rainbow," a flat analog of the dispersive prism in optics. The proposed scheme of hybrid system involving graphene for dynamic control of G–H shift will have potential applications in the manipulation of terahertz waves.

1. Introduction

In recent years, there has been enormous scientific interest on graphene, a type of 2D crystal with carbon atoms arranged in a honeycomb lattice.[1] Graphene is attractive for both its novel physical properties (e.g., the unusual quantum Hall effect)[2,3] and myriad applications that profit from its high electronic mobility,[4] exceptional mechanical strength,[5] and thermal conductivity.[6] Graphene is also promising for applications in photonics and optoelectronics.[7] Compared to regular bulk metals, the surface plasmons in graphene show much stronger confinement of plasmonic excitations at the atomic scale,[8] which implies that graphene is a novel platform for boosting light–matter interactions with the excitation of surface plasmons.[9] More importantly, the low carrier concentration in graphene sheet provides ultra-wide tunable space in responding to external stimuli.[10] Low plasma frequency and ultra-wide range tunability make it a feasible and outstanding optical material for actively controllable plasmonic metamaterials/metasurfaces[11] especially for terahertz (THz) and far-infrared applications.[10,12–14] The graphene metasurfaces provide possibilities to realize tailorable functionalities in transformation optics,[15] surface cloak,[16] plasmonic waveguides,[17–19] optical modulators,[20–22] and absorbers.[23–28] Some recent studies opened up the possibility of realizing dynamic manipulation of light beams by exploiting the gate-controllable optical properties of graphene.[29–32]

Goos–Hänchen (G–H) effect,[33] the lateral shift of a reflected light beam with respect to the prediction of geometric optics, is an interesting phenomenon. The G–H effect originates from angularly dispersive phase delay of light beam, various material systems and structures, such as dielectric slab,[34] absorbing media and metals,[35–39] photonic crystals,[40] and metamaterials,[41–43] have been employed to modify the phase delay and thus the G–H effect. The G–H shift has been applied for chemical sensor, detection of displacement, refraction index, and irregularities or surface roughness, which are important in modern science. Predictably, achieving efficient tunability in G–H shifts with external stimuli like electrical signal will extend the research scope of G–H effect as well as corresponding applications. In this article, we propose a mechanism

Prof. Y. Fan, Prof. F. Zhang, Dr. Q. Fu
Key Laboratory of Space Applied Physics and Chemistry
Ministry of Education and Department of Applied Physics
School of Science
Northwestern Polytechnical University
Xi'an 710129, China
E-mail: phyfan@nwpu.edu.cn

Dr. N.-H. Shen, P. Zhang, Dr. T. Koschny, Prof. C. M. Soukoulis
Ames Laboratory and Department of Physics and Astronomy
Iowa State University
Ames, IA 50011, USA

Prof. Z. Wei, Prof. H. Li
Key Laboratory of Advanced Micro-structure Materials (MOE)
and School of Physics Science and Engineering
Tongji University
Shanghai 200092, China

Prof. Q. Zhao
State Key Laboratory of Tribology
Department of Mechanical Engineering
Tsinghua University
Beijing 100084, China

Prof. C. M. Soukoulis
Institute of Electronic Structure and Laser
FORTH
71110 Heraklion, Crete, Greece

Materials
Views
www.MaterialsViews.com

ADVANCED
OPTICAL
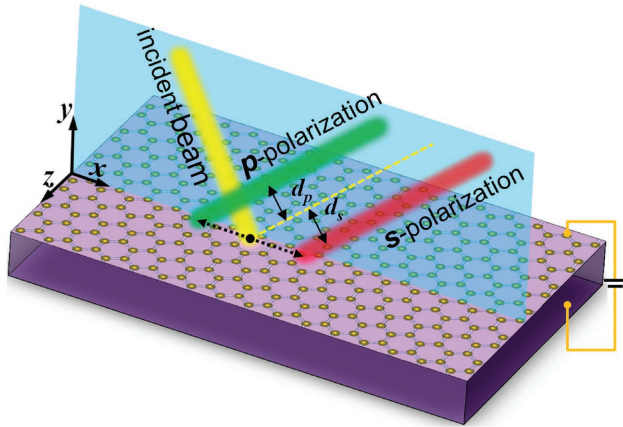MATERIALS
www.advopticalmat.de

FULL PAPER

Figure 1. Schematic of the investigated system: a graphene covered epsilon-near-zero (ENZ) metamaterial substrate is irradiated by the terahertz beams from the air side, s-polarized/p-polarized beams show positive/negative Goos–Hänchen (G–H) shifts under oblique incidence.

to achieve electrically tailorable G–H shifts in photonic systems by utilizing the tunable optical properties of graphene.

For simplicity and without loss of generality, we consider a basic 1D system (see **Figure 1**), in which a monolayer graphene, which will be electrically biased for tunability, is settled on top of a substrate, and the whole architecture is irradiated by THz beams from the top (air) side. In our system, the substrate is taken with a special category of metamaterials, i.e., an epsilon-near-zero (ENZ) medium, which is fairly easy in the design and more importantly, can efficiently reflect the impinging THz beam so as to greatly benefit the observation of G–H shift.[43] It is noteworthy that near-zero metamaterials[44–47] and graphene–metamaterial hybrid systems[48,49] are interesting in wave manipulations, which have been experimentally demonstrated in various configurations at the microwave, THz, infrared, and even visible frequencies. In the study, we found that the G–H shifts of THz beams can be either positive or negative for different polarizations, and the G–H shift can be tuned substantially by controlling the Fermi level of the monolayer graphene. And in addition, the wavelength-dependent G–H shift of the graphene/metamaterial hybrid system benefits potential functionalities like "rainbow" for THz application as a planar analog of the dispersive prism.

2. Results and Discussion

We assigned the electromagnetic parameters for the ENZ metamaterial substrate to be $\varepsilon_{sub} = 10^{-2} + 0.01i$ and $\mu_{sub} = 1$,[43] and employed a transfer matrix method (TMM)[50–52] to analyze the scattering properties of the system, which is suitable for the study of layered systems. The novel contributions of the monolayer graphene can be taken into account in the TMM by considering additional scatterings originated from the surface conductivity σ of it in the transfer matrix

$$M_t(\omega, \theta) = \frac{1}{2} \begin{bmatrix} 1+\eta+\varsigma & 1-\eta-s\varsigma \\ 1-\eta+s\varsigma & 1+\eta-\varsigma \end{bmatrix} \tag{1}$$

with $\eta = \frac{k_{sub,y}}{k_{air,y}}$ $\left(\eta = \frac{\varepsilon_{air}k_{sub,y}}{\varepsilon_{sub}k_{air,y}} \right)$ being the conventional contribution of dielectric films and $\varsigma = \frac{\sigma\mu_0\omega}{k_{air,y}}$ $\left(\varsigma = \frac{\sigma k_{sub,y}}{\varepsilon_0\varepsilon_{sub}\omega} \right)$ the contribution from the surface conductivity of 2D materials for the s-polarized (p-polarized) light, s equals $1(-1)$ for p-polarization (s-polarization). $k_{air(sub),y}$ is the y-component of the wave vector $k_{air(sub)} = \sqrt{\varepsilon_{air(sub)}}\omega/c$ in air (substrate), where ω is the angular frequency, c is the speed of light in vacuum, and θ is the angle of wave vector with respect to y-axis. ε_0 and μ_0 are vacuum permittivity and permeability, respectively. Since we mainly consider the scatterings of graphene involved interface in this paper, the propagating matrix in the substrate is $M_p(\omega, \theta) = \text{diag}(1,1)$, and thus the transfer matrix of the whole system should be

$$T(\omega, \theta) = \sum M_t M_p = M_t \tag{2}$$

The reflection coefficients of the considered system are then given by the elements of transfer matrix

$$r = \frac{T_{21}}{T_{11}} = \frac{1-\eta+s\varsigma}{1+\eta+\varsigma} \tag{3}$$

With respect to the crucial parameter, i.e., complex surface conductivity σ, of the graphene in our modeling, it can be given as the following expression in the theoretical perspective based on random phase approximation in the local limit

$$\sigma = \frac{e^2 E_F}{\pi\hbar^2} \frac{i}{\omega + i\tau^{-1}} + \frac{e^2}{4\hbar} \left[\theta(\hbar\omega - 2E_F) + \frac{i}{\pi} \log \left| \frac{\hbar\omega - 2E_F}{\hbar\omega + 2E_F} \right| \right] \tag{4}$$

in which E_F represents the Fermi energy, $\tau = \mu E_F / e v_F^2$ is the relaxation rate with the mobility $\mu = 10^4$ cm^2 Vs^{-1}, and Fermi velocity $v_F \approx 10^6$ ms^{-1}. The first and the second terms at the right side of Equation (2) correspond to intra-band processes and inter-band transitions, respectively, in a monolayer graphene. The scattering coefficients of the system can then be obtained by plugging the dispersive surface conductivity into the transfer matrix.

There have been quite a few attempts to theoretically account the G–H shift.[53–55] One of the most well-accepted theoretical explanations for G–H shift is via the picture of stationary phase approximation,[53,54] in which, the G–H shift d is given by

$$d = -\frac{\lambda}{2\pi} \frac{\partial\varphi(\theta_i)}{\partial\theta_i} \tag{5}$$

where λ is the wavelength of terahertz beam, and the phase $\varphi(\theta_i)$ of reflection coefficient r is a function of the incident angle θ_i. Therefore, it is straightforward that, by applying Equations (1)–(4) to Equation (5), we can calculate the G–H shift of the system. Due to the complexity of the direct expression,
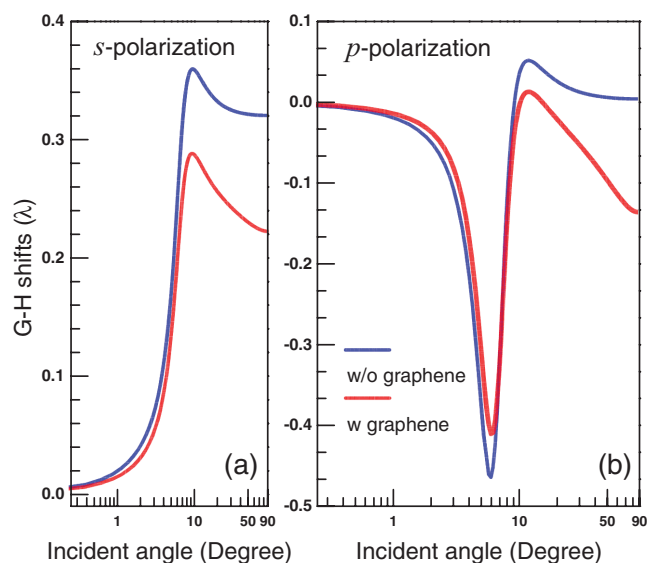
Figure 2. Comparison of the G–H shifts of an ENZ metamaterial substrate with (red) and without (blue) the graphene (Fermi energy: 0.5 eV) cover. Calculated G–H shifts versus incident angle of the a) s-polarized and b) p-polarized terahertz beams at 8 THz.

Figure 3. Comparison of the G–H shifts of an ENZ metamaterial substrate with a graphene (Fermi energy: 0.5 eV) cover at different frequencies (3, 5, 10, and 35 THz). Calculated G–H shifts versus incident angle of the a) s-polarized and b) p-polarized terahertz beams.

which does not provide us additional insight, we would like to directly study the G–H effect in our hybrid system numerically.

The angular spectra of the G–H shift for the orthogonal s-polarized and p-polarized beams at 8 THz are shown in **Figure 2**, where logarithmic scaled angular x-axis was used for clearly showing the results. For the cases without graphene layer, the G–H shifts are about 0.32λ and 0 in a wide range of oblique incidence for s-polarized and p-polarized beams, respectively, indicated with blue lines in Figure 2. The dispersive behavior at small angle of incidence is due to loss-induced phase change from near linearly changing phase of reflection coefficients of the ENZ medium.[43] In contrast, red lines in Figure 2 show the G–H shifts for the hybrid system with the graphene layer included, where the Fermi energy of graphene was taken as $E_F = 0.5\,\mathrm{eV}$. We can see, with the introduction of the monolayer graphene, the G–H shift at large incidence angles, or the angular flat range for the substrate, undergoes an angular-dependent change. Comparing the cases with and without the graphene layer, the G–H shifts at small incidence angles (less than $\approx 10°$) are almost not changed, and the relatively larger G–H shifts at large incidence angles are of more interest: for s-polarization, the doped graphene on the substrate decreases the G–H shift, and such a change slightly increases with the increase of incidence angle; for p-polarization, the absolute value of the negative G–H shift increases when the angle of incidence gets larger. The opposite sign of the G–H shifts under different polarizations, combining the electrically tunable response of graphene, will benefit the manipulation of the THz beams, as shown below.

As can be seen from Figure 2, the G–H shift of a photonic system can be significantly tailored with the contribution of surface conductivity of a monolayer graphene, which is intrinsically dispersive as that showed in Equation (4). Therefore, it is conceivable that the frequency-dependent modification of graphene will show distinct dispersive behavior on the G–H shift
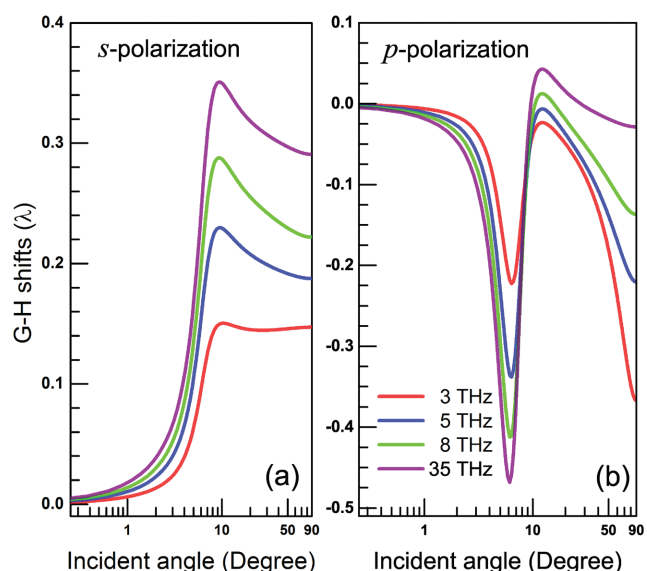
in the hybrid system. The angular spectra of the G–H shift for the s-polarized and p-polarized beams of different frequencies (3, 5, 10, and 35 THz) are shown in **Figure 3** a,b for comparison, the Fermi energy of graphene is $E_F = 0.5\,\mathrm{eV}$. For s-polarization, the changes in G–H shift at small incident angles are very limited, so we mainly focus on the frequency dispersion at large angles of incidence: the G–H shift spectrum stays fairly flat at 3 THz, and upon the increase of the frequency, the values of the plateaus do increase gradually, and the G–H shift spectrum finally gets closer and comparable to the case without graphene (see the blue curve in Figure 2a). For p-polarization as shown in Figure 3b, the frequency-dependent response is more complicated. The loss in the ENZ substrate induces a resonant behavior around the pseudo-Brewster angle, which shows an abrupt reflection phase change and thus resonant and negative G–H shifts under small incidence angles. The THz complex surface conductivity of doped graphene is mainly contributed from the Drude term [the first term in Equation (4)], corresponding to the intra-band processes in graphene, the Drude line-shaped complex conductivity is of different lossy rate ($\mathrm{Re}[\sigma]/\mathrm{Im}[\sigma]$). The graphene can significantly influence the resonant strength on G–H shift. While for larger incident angles, the frequency dependence shows similar behavior as that of s-polarization, i.e., the negative G–H shift finally gets very closer to the case without graphene at high frequencies. Potentially, the opposite directions of beam shift for different polarizations may provide a strategy of beam splitting. However, it is noteworthy that such a prototype effect in our simplified system is only on the order of one wavelength and a detectable corresponding beam splitting effect may need some more complicated configurations based on our proposal, for instance, the multiple scatterings in layered structure[34,40] and total internal reflection (TIR).[56] Furthermore, the converging dispersion of the G–H shift at oblique angles can serve as an implementation
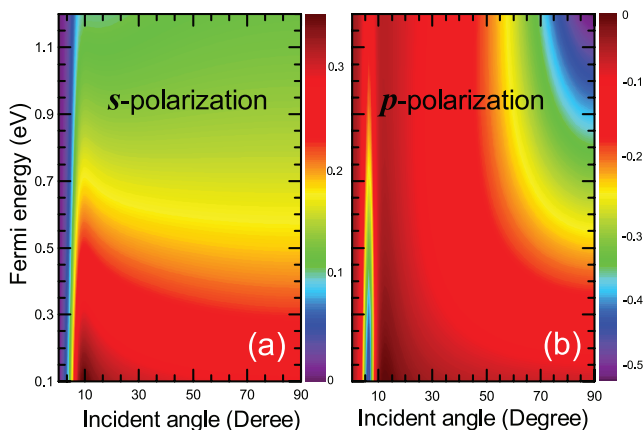
Figure 4. G–H shift angular spectra of the orthogonal a) s-polarized and b) p-polarized terahertz beams at 5 THz for graphene sheet with different Fermi energy (from 0.1 to 1.2 eV).

of a "rainbow"-like function for THz radiations, a flat analog to the classical dispersive prism in optics.

To further investigate the tunability of G–H shift assisted by the doped graphene, we calculated the G–H shift spectra for graphene under various Fermi energies ranging from 0.1 to 1.2 eV, with the frequency set at 5.0 THz. The false-color maps of the G–H shifts versus Fermi energies and incident angles are plotted in **Figure 4** a,b for s- and p-polarization, respectively. With increasing Fermi energy, we found more remarkable modification in G–H shifts with respect to that of sole-substrate system for both polarizations. The boosting of modification on G–H shift for higher Fermi energy can be understood as follows: the mainly contributed Drude term from intra-band transitions at a fixed frequency is stronger for graphene with higher Fermi energy, so the scattering coming from the graphene gets more dramatic, leading to an efficient modification in G–H shift with wide-range tunability. Therefore, the electrical doping can tune the optical properties of graphene toward a notable modification in G–H shift, and conversely, such an effect also provides us a strategy to monitor doping level or Fermi energy of graphene sample.

Finally, we performed full-wave numerical simulations to our hybrid system with graphene to show the G–H shifts intuitively, as a verification of our theoretical predictions in the above. The simulations were finished via COMSOL, a commercial electromagnetic software package based on the finite element method, in which, the graphene layer was modeled as a 2D "surface current" sheet with complex surface conductivity, the values employed in the theoretical analysis at $E_F = 0.5\text{eV}$ are directly applied in COMSOL. The angle of incidence for both polarizations is 45° with the waist of beam set to be 3λ as indicated in **Figure 5**c, as can be seen from the lateral profiles (normalized to the wavelength λ, s-polarization: blue solid line; p-polarization: yellow dashed line) of the time-averaged power flow in Figure 5c. The out-of-plane field components are captured and plotted in Figure 5a ($|\mathbf{E}_z|$ for s-polarization at 10 THz) and Figure 5b ($|\mathbf{H}_z|$ for p-polarization at 3 THz), respectively. From the field maps in Figure 5, we can get the lateral shift of reflected beams from center of the specular reflection, and the G–H shifts are shown to be positive (negative) for s- (p-) polarized beams, more clearly according to the cross-section profiles of power
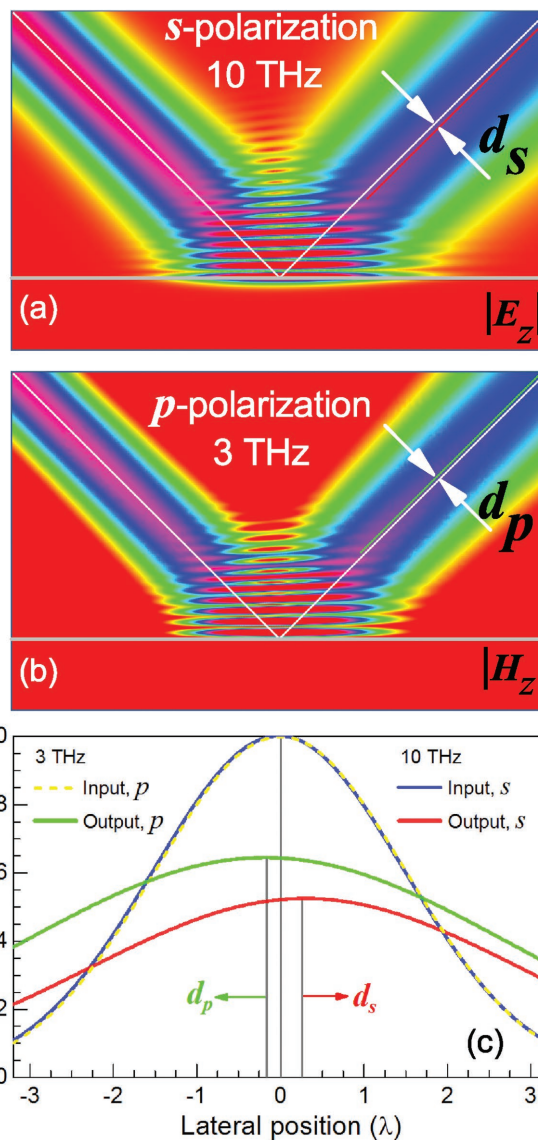

Figure 5. Numerical verification of the theoretically predicted G–H effect: Map of the out-of-plane electromagnetic components and time-averaged power flow of the input/output terahertz beams with different polarizations, Fermi energy of graphene: 0.5 eV. a) Electric and b) magnetic field patterns for s-polarized (10 THz) and p-polarized (3 THz) beams at the incident angle of 45°, the G–H shifts are denoted by white arrows. c) Cross-section profiles of the normalized power flow of the input and reflected beams.

flow (see Figure 5c). From the simulations, G–H shifts for s- and p-polarization are $d_s = 0.259\lambda$ and $d_p = -0.160\lambda$, respectively, which agree well with the theoretical predictions of TMM analysis, i.e., $d_s = 0.247\lambda$ and $d_p = -0.155\lambda$.

3. Conclusion

In conclusion, we proposed a strategy to realize controllable G–H shifts in the THz regime by taking advantage of the fascinating tunable properties of graphene. For a simple

FULL PAPER

modeling system with graphene settled on top of an ENZ medium, we have theoretically and numerically studied the tunability and the dependency of G–H shifts with respect to Fermi energy of graphene, frequency, and polarization state of the THz beam. The proposed graphene-assisted hybrid system benefits potential functionalities in the manipulation of THz waves, such as the "rainbow"-like dispersion, a planar analog of dispersive prisms. The demonstrated tunable G–H shifts can also serve as a strategy to determine the doping level (Fermi energy) of graphene layer reversely. Finally, we emphasize that the mechanism proposed in this paper is not limited to graphene, but also applicable to the 2D conductive material category, which is a hotspot in optics and photonics recently.

[1] A. K. Geim, *Science* **2009**, *324*, 1530.
[2] K. S. Novoselov, A. K. Geim, S. V. Morozov, D. Jiang, M. I. Katsnelson, I. V. Grigorieva, S. V. Dubonos, A. A. Firsov, *Nature* **2005**, *438*, 197.
[3] Y. Zhang, Y.-W. Tan, H. L. Stormer, P. Kim, *Nature* **2005**, *438*, 201.
[4] S. V. Morozov, K. S. Novoselov, M. I. Katsnelson, F. Schedin, D. C. Elias, J. A. Jaszczak, A. K. Geim, *Phys. Rev. Lett.* **2008**, *100*, 016602.
[5] C. Lee, X. Wei, J. W. Kysar, J. Hone, *Science* **2008**, *321*, 385.
[6] A. A. Balandin, S. Ghosh, W. Bao, I. Calizo, D. Teweldebrhan, F. Miao, C. N. Lau, *Nano Lett.* **2008**, *8*, 902.
[7] F. Bonaccorso, Z. Sun, T. Hasan, A. C. Ferrari, *Nat. Photonics* **2010**, *4*, 611.
[8] A. N. Grigorenko, M. Polini, K. S. Novoselov, *Nat. Photonics* **2012**, *6*, 749.
[9] F. H. L. Koppens, D. E. Chang, F. J. G. de Abajo, *Nano Lett.* **2011**, *11*, 3370.
[10] T. Low, P. Avouris, *ACS Nano* **2014**, *8*, 1086.
[11] H.-T. Chen, J. F. O'Hara, A. K. Azad, A. J. Taylor, R. D. Averitt, D. B. Shrekenhamer, W. J. Padilla, *Nat. Photonics* **2008**, *2*, 295.
[12] L. Ju, B. Geng, J. Horng, C. Girit, M. Martin, Z. Hao, H. A. Bechtel, X. Liang, A. Zettl, Y. R. Shen, F. Wang, *Nat. Nanotechnol.* **2011**, *6*, 630.
[13] P. Tassin, T. Koschny, C. M. Soukoulis, *Science* **2013**, *341*, 620.
[14] Y. Fan, N.-H. Shen, T. Koschny, C. M. Soukoulis, *ACS Photonics* **2015**, *2*, 151.
[15] A. Vakil, N. Engheta, *Science* **2011**, *332*, 1291.
[16] P.-Y. Chen, A. Alù, *ACS Nano* **2011**, *5*, 5855.
[17] M. Jablan, H. Buljan, M. Soljačić, *Phys. Rev. B* **2009**, *80*, 245435.

[18] S. He, X. Zhang, Y. He, *Opt. Express* **2013**, *21*, 30664.
[19] A. Woessner, M. B. Lundeberg, Y. Gao, A. Principi, P. Alonso-González, M. Carrega, K. Watanabe, T. Taniguchi, G. Vignale, M. Polini, J. Hone, R. Hillenbrand, F. H. L. Koppens, *Nat. Mater.* **2015**, *14*, 421.
[20] Y. Zou, P. Tassin, T. Koschny, C. M. Soukoulis, *Opt. Express* **2012**, *20*, 12198.
[21] X. Gan, R.-J. Shiue, Y. Gao, K. F. Mak, X. Yao, L. Li, A. Szep, D. Walker, J. Hone, T. F. Heinz, D. Englund, *Nano Lett.* **2013**, *13*, 691.
[22] Y. Yao, R. Shankar, M. A. Kats, Y. Song, J. Kong, M. Loncar, F. Capasso, *Nano Lett.* **2014**, *14*, 6526.
[23] S. Thongrattanasiri, F. H. L. Koppens, F. J. G. de Abajo, *Phys. Rev. Lett.* **2012**, *108*, 047401.
[24] R. Alaee, M. Farhat, C. Rockstuhl, F. Lederer, *Opt. Express* **2012**, *20*, 28017.
[25] Y. Fan, Z. Wei, Z. Zhang, H. Li, *Opt. Lett.* **2013**, *38*, 5410.
[26] M. S. Jang, V. W. Brar, M. C. Sherrott, J. J. Lopez, L. Kim, S. Kim, M. Choi, H. A. Atwater, *Phys. Rev. B* **2014**, *90*, 165409.
[27] Y. Fan, Z. Liu, F. Zhang, Q. Zhao, Z. Wei, Q. Fu, J. Li, C. Gu, H. Li, *Sci. Rep.* **2015**, *5*, 13956.
[28] Y. Xiang, X. Dai, J. Guo, H. Zhang, S. Wen, D. Tang, *Sci. Rep.* **2014**, *4*, 5483.
[29] F. Lu, B. Liu, S. Shen, *Adv. Opt. Mater.* **2014**, *2*, 794.
[30] C. Eduardo, T. Michele, R. M. Juan, L. Tony, P.-C. Julien, *Nanotechnology* **2015**, *26*, 134002.
[31] Z. Li, K. Yao, F. Xia, S. Shen, J. Tian, Y. Liu, *Sci. Rep.* **2015**, *5*, 12423.
[32] H. Cheng, S. Chen, P. Yu, W. Liu, Z. Li, J. Li, B. Xie, J. Tian, *Adv. Opt. Mater.* **2015**, *3*, 1744.
[33] F. Goos, H. Hänchen, *Ann. Phys.* **1947**, *436*, 333.
[34] C.-F. Li, *Phys. Rev. Lett.* **2003**, *91*, 133903.
[35] W. J. Wild, C. L. Giles, *Phys. Rev. A* **1982**, *25*, 2099.
[36] H. M. Lai, S. W. Chan, *Opt. Lett.* **2002**, *27*, 680.
[37] L.-G. Wang, H. Chen, S.-Y. Zhu, *Opt. Lett.* **2005**, *30*, 2936.
[38] P. T. Leung, C. W. Chen, H. P. Chiang, *Opt. Commun.* **2007**, *276*, 206.
[39] M. Merano, A. Aiello, G. W. 't Hooft, M. P. van Exter, E. R. Eliel, J. P. Woerdman, *Opt. Express* **2007**, *15*, 15928.
[40] I. V. Soboleva, V. V. Moskalenko, A. A. Fedyanin, *Phys. Rev. Lett.* **2012**, *108*, 123901.
[41] P. R. Berman, *Phys. Rev. E* **2002**, *66*, 067603.
[42] I. V. Shadrivov, A. A. Zharov, Y. S. Kivshar, *Appl. Phys. Lett.* **2003**, *83*, 2713.
[43] Y. Xu, C. T. Chan, H. Chen, *Sci. Rep.* **2015**, *5*, 8681.
[44] A. M. Mahmoud, N. Engheta, *Nat. Commun.* **2014**, *5*.
[45] X. Huang, Y. Lai, Z. H. Hang, H. Zheng, C. T. Chan, *Nat. Mater.* **2011**, *10*, 582.
[46] R. Maas, J. Parsons, N. Engheta, A. Polman, *Nat. Photonics* **2013**, *7*, 907.
[47] Q. Zhao, Z. Xiao, F. Zhang, J. Ma, M. Qiao, Y. Meng, C. Lan, B. Li, J. Zhou, P. Zhang, N.-H. Shen, T. Koschny, C. M. Soukoulis, *Adv. Mater.* **2015**, *27*, 6187.
[48] J. Li, Y. Zhou, B. Quan, X. Pan, X. Xu, Z. Ren, F. Hu, H. Fan, M. Qi, J. Bai, L. Wang, J. Li, C. Gu, *Carbon* **2014**, *78*, 102.
[49] Z. Miao, Q. Wu, X. Li, Q. He, K. Ding, Z. An, Y. Zhang, L. Zhou, *Phys. Rev. X* **2015**, *5*, 041027.
[50] C. S. R. Kaipa, A. B. Yakovlev, G. W. Hanson, Y. R. Padooru, F. Medina, F. Mesa, *Phys. Rev. B* **2012**, *85*, 245407.
[51] T. Zhan, X. Shi, Y. Dai, X. Liu, J. Zi, *J. Phys.: Condens. Matter* **2013**, *25*, 215301.
[52] Y. Fan, Z. Wei, H. Li, H. Chen, C. M. Soukoulis, *Phys. Rev. B* **2013**, *88*, 241403(R).
[53] K. Artmann, *Ann. Phys.* **1948**, *437*, 87.
[54] K. W. Chiu, J. J. Quinn, *Am. J. Phys.* **1972**, *40*, 1847.
[55] R. H. Renard, *J. Opt. Soc. Am.* **1964**, *54*, 1190.
[56] X. Li, P. Wang, F. Xing, X.-D. Chen, Z.-B. Liu, J.-G. Tian, *Opt. Lett.* **2014**, *39*, 5574.